

# ACCELERATOR PHYSICS ISSUES FOR FUTURE ELECTRON-ION COLLIDERS

S. Peggs, I. Ben-Zvi, J. Kewisch, J. Murphy, BNL.

## 1 INTRODUCTION

Interest continues to grow in the physics of collisions between electrons and heavy ions, and between polarized electrons and polarized protons [1, 2, 3]. Table 1 compares the parameters of some machines under discussion. DESY has begun to explore the possibility of upgrading the existing HERA-p ring to store heavy ions, in order to collide them with electrons (or positrons) in the HERA-e ring, or from TESLA [4]. An upgrade to store polarized protons in the HERA-p ring is also under discussion [1]. BNL is considering adding polarized electrons to the RHIC repertoire, which already includes heavy and light ions, and polarized protons. The authors of this paper have made a first pass analysis of this “eRHIC” possibility [5]. MIT-BATES is also considering electron ion collider designs [6].

**Ring-Ring and Linac-Ring scenarios.** Figure 1 compares the *ring-ring* and *linac-ring* scenarios, using eRHIC as a convenient example. In the “*ring-ring*” scenario (TOP), pre-polarized electrons are injected into an electron storage ring from a full energy linac (or from a booster). Collisions are possible with the clockwise rotating ions at up to 5 interaction points. The average electron beam power passing a single point – a few GW – is contained as a stored beam energy which is conserved except for synchrotron radiation losses of about 1 MW. In the *linac-ring* scenario (BOTTOM) the beam circulates only once, before the average electron beam power – about 1 GW – is recovered by passing the beam back through the linac. The recirculation ring may, or may not, share a tunnel with the ion ring. The Energy Recovery Linac (ERL) must be superconducting in a *linac-ring* design, constructed of niobium superconducting cavities (for example using 1.3 GHz TESLA cavities). In the *ring-ring* scenario the linac could alternately be constructed with copper cavities (for example at the SLAC linac frequency of 2.856 GHz, where cavities and RF sources are readily available). Such a copper linac has no particularly new issues or difficulties, except in the need for an electron gun which can provide polarized electrons at up to 80% polarization [7, 8].

## 2 ULTIMATE PERFORMANCE

The luminosity is given by

$$L = F_c \frac{N_e N_i}{4\pi\sigma^{*2}} \quad (1)$$

where  $F_c = 1/\tau_{bunch}$  is the collision frequency,  $N_e$  and  $N_i$  are the single bunch populations for electrons and ions, and  $\sigma^*$  is the round beam collision size (assumed to be the

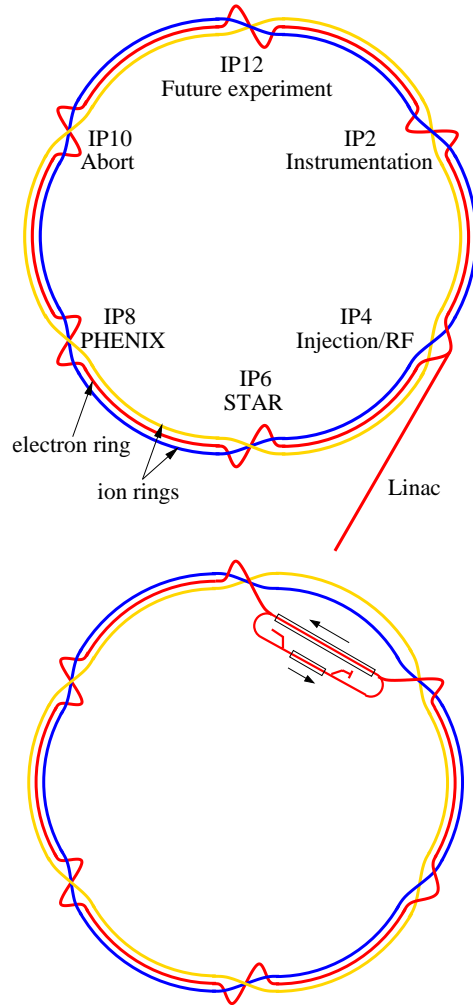


Figure 1: In the *ring-ring* scenario (TOP) electrons are stored for hours in their own ring. In the *linac-ring* scenario (BOTTOM) electrons circulate the ring once, before re-entering the superconducting Energy Recovery Linac.

same for both beams). The RMS electron and ion beam sizes are written as

$$\sigma_i^* = \sqrt{\frac{\beta_i^* \epsilon_i}{(\beta\gamma)_i}} \quad (2)$$

$$\sigma_e^* = \sqrt{\beta_e^* \epsilon_e} \quad (3)$$

where  $\epsilon_i$  is the *normalized* RMS ion emittance (no  $4\pi$  or  $6\pi$ ), and where the electron emittance  $\epsilon_e$  is *unnormalized*.

The electron and ion beam-beam parameters  $\xi_e$  and  $\xi_i$  depend *only* on the bunch population of the other beam,

Table 1: Future electron-ion collider design study parameters. The SLAC HER is included for comparison purposes.

	<b>THERA</b>	<b>EPIC</b>	<b>eRHIC</b>	<b>eRHIC</b>	<b>SLAC HER</b>
Scenario	linac-ring	linac-ring	linac-ring	ring-ring	(B-factory)
Ion specie	protons	protons	protons/gold	protons/gold	–
Luminosity, [ $10^{32} \text{cm}^{-2} \text{s}^{-1}$ ]	.041	21	4.6/.036	3.5/.086	–
Ring circumference, [m]	6355	500	3833	3833	2200
Dipole bend radius, [m]	608	$\sim 50$	243	243	165
RMS beam size, $\sigma^*$ [ $\mu\text{m}$ ]	10	25	21/60	40/50	157
Bunch spacing, [ns]	211	6.7	35.5	35.5	4.2
<b>ION PARAMETERS</b>					
Ion energy, [GeV/u]	1,000	50	250/100	250/100	–
Electron cooling?	no	yes	yes	yes	–
Ion emittance, norm. RMS, [ $\mu\text{m}$ ]	1.0	2.0	0.8/1.0	0.8/1.0	–
Ions per bunch, $N_i$ [ $10^{11}$ ]	1.0	1.0	.3/.019	.94/.012	–
Ion average current, [A]	.071	2.4	.14/.68	.42/.42	–
Ion IP beta, $\beta_e^*$ [m]	.10	.10	.15/.39	.53/.27	–
Ion angular beam size, $\sigma_i'^*$ [ $\mu\text{r}$ ]	100	250	143/155	75/186	–
Ion bunch length, [m]	.10	.10	.1/.3	.1/.2	–
Ion beam-beam parameter, $\xi_i$	.0023	.004	.0046/.0015	.004/.004	–
Laslett space charge tune shift, $\Delta Q$	.0003	.024	.001/.003	.003/.003	–
<b>ELECTRON PARAMETERS</b>					
Electron energy, [GeV]	250	5	10	10	9
Electron emittance, [nm]	.2	6	3	18	49
Electrons per bunch, $N_e$ [ $10^{11}$ ]	.2	.11	.3/.3	.26/.81	.56
Electron average current, [A]	.000084	.264	.135/.135	.12/.37	1.5
Electron IP beta, $\beta_e^*$ [m]	.50	.10	.15/1.2	.089/.139	.05/.50
Electron angular beam size, $\sigma_e'^*$ [ $\mu\text{r}$ ]	20	250	143/50	450/360	313
Electron bunch length, [mm]	.3	1	3	9	11
Electron beam-beam parameter, $\xi_e$	.23	.35	.11/.57	.06/.06	.055
Electron average power, [GW]	.023	1.32	1.35/1.35	1.2/3.7	13.5
Synch. radiation power, [MW]	–	$\sim .29$	.49/.49	.43/1.3	7.2
Linear synch. power, [kW/m]	–	$\sim .93$	.32/.32	.28/.87	5.1

and the emittance (at constant energy). They are given by

$$\xi_e = \frac{N_i}{\epsilon_e} \left( \frac{r_e Z}{4\pi\gamma_e} \right) \quad (4)$$

$$\xi_i = \frac{N_e}{\epsilon_i} \left( \frac{r_i (v/c)_i}{4\pi Z} \right) \quad (5)$$

where  $r_i$ , the classical radius of the ion

$$r_i = \frac{Z^2 e^2}{A 4\pi\epsilon_0 M_0 c^2} \quad (6)$$

is  $r_p = 1.53 \times 10^{-18}$  m for protons,  $r_{Au} = 49.0 \times 10^{-18}$  m for gold, and  $r_e = 2.82 \times 10^{-15}$  m for electrons. The critical values for  $\xi_e$  and  $\xi_i$  which cannot be surpassed for circulating beams are approximately

$$\xi_e \leq 0.06 \quad \text{and} \quad \xi_i \leq 0.004 \quad (7)$$

(In the linac-ring scenario the electrons are “thrown away” after one turn, and this limit on  $\xi_e$  can be violated.)

The interaction region optics are characterized by the maximum angular beam size at the IP

$$\sigma_i'^* = \frac{\sigma^*}{\beta^*} \leq \frac{1}{n} \frac{a}{\hat{d}} \quad (8)$$

where  $n$  ( $\approx 6$  for ions and  $\approx 12$  for electrons) is the number of beam sigmas which must fit in  $a$ , the aperture of the interaction region (IR) quads, and the “effective IR aperture distance”  $\hat{d}$  is defined by

$$\hat{d} = \sqrt{\hat{\beta}\beta^*} \quad (9)$$

where  $\hat{\beta}$  is the maximum beta function. Both  $\hat{d}$  and the maximum angular beam size are almost independent of  $\beta^*$  (for non-pathological optics). The luminosity may now be written

$$L = F_c \xi_e \xi_i \sigma_e'^* \sigma_i'^* \left( \frac{4\pi\gamma_e \gamma_i}{r_e r_i} \right) \quad (10)$$

This parameterization is useful when the luminosity performance is simultaneously limited, or nearly limited, by beam-beam effects and by interaction region optics, since then the values of  $\xi$  and  $\sigma'^*$  are well known. It is implicitly assumed that  $N/\epsilon$  and  $\beta^*$  values can be tuned appropriately (to reach  $\xi$  and  $\sigma'^*$  limits, respectively).

**Number of bunches, bunch spacing.** If the beam-beam parameters and the angular beam sizes are already

at their limits, the only way to raise the luminosity is to increase the collision frequency  $F_c$ , by increasing  $M$ , the number of bunches. One constraint on  $M$  is the maximum average current. Another is the need for a minimum bunch spacing – perhaps due to the electron cloud effect, or due to a minimum reset time for detector electronics. In an electron ring the average current may be limited by the total synchrotron radiation load, or by the heat load per meter. In a superconducting ion ring the beam image current which flows in the vacuum chamber walls is a resistive heat load at cryogenic temperatures. A maximum average cryogenic heat load of about 1 W/m can be tolerated, to stay within the capacity of typical cryogenic systems. Beam Position Monitor signal cables may suffer unacceptably large cold-to-warm heat loads, due to resistive heating by the signal current, when the number of bunches becomes large and the bunches are too short [10].

### 3 ION STORAGE RING ISSUES

**Long range beam-beam.** It is relatively easy to immunize an electron ion collider against parasitic long range beam-beam interactions, by arranging for the early separation of the two beams (with very unequal rigidities). For example, in eRHIC the beams begin to be magnetically separated at only 9.8 meters from the IP, before entry into the first quadrupole, and after only one parasitic interaction.

**Electron cloud effect.** Electrons produced by ionization of the residual gas are accelerated by the electrical field of the next passing ion bunch, eventually hitting the vacuum chamber wall and emitting secondary electrons. This process can runaway if the bunches are spaced too closely, driving a large cryogenic heat load in a superconducting ion ring and perhaps causing instabilities. The effect has been much studied for the LHC, where the nominal bunch spacing is 25 ns and there are nominally about  $10^{11}$  protons per bunch [11, 12, 13]. In fixed target mode the Tevatron routinely operates with 1008 bunches of approximately  $2 \times 10^{10}$  protons, spaced by about 18.9 ns (53 MHz), without undue cryogenic difficulty. Bunch gaps – such as the 1  $\mu$ s abort gap in the Tevatron – act to clear the electron clouds. Unfortunately there is a paucity of hard experimental data from existing cryogenic accelerators with closely spaced bunches, although the normal conducting SPS is generating interesting data with LHC bunch loading parameters. This problem needs more investigation, especially in making careful measurements on cryogenic storage rings – HERA, RHIC, the Tevatron – and in the SPS.

**Intra-Beam Scattering (IBS) and electron cooling.** Intra Beam Scattering diffusion can be very strong for heavy ions such as gold. For example, in RHIC the normalized emittance is expected to grow from about 2  $\mu$ m to about 7  $\mu$ m in a ten hour store with  $10^9$  ions per bunch. As a rule, the effect is stronger at lower energies. Electron coolers can fight IBS, even reducing the emittance below

its injection value. For example, the RHIC gold emittance is predicted to shrink to about 1  $\mu$ m after 1 hour in a proposed e-cooling upgrade scheme [14, 15].

**Laslett space charge tune shift.** The space charge tune shift of the ion beam is given by

$$\Delta Q_{sc} \approx -\frac{N_i}{\epsilon_i} \frac{C}{\sigma_L \beta \gamma^2} \left( \frac{r_i}{2(2\pi)^{3/2}} \right) \quad (11)$$

Although its dependence on  $N/\epsilon$  is reminiscent of the beam-beam parameter, in contrast is the strong dependence on ring circumference  $C$ , RMS bunch length  $\sigma_L$ , and the Lorentz factors  $\beta$  and  $\gamma$ . Because the space charge interaction is “smoothly” spread over the circumference of the ring, resonances tend to be only weakly driven, and so values as large as  $\Delta Q_{sc} \approx 0.1$  can reasonably be supported. At constant bunch length space charge is much more of a problem at injection, when  $\beta\gamma^2$  is smallest. However, it is possible to make the bunch much longer at injection. For example, eRHIC injects and accelerates with a 28 MHz RF system, but stores beam for collisions with a 197 MHz RF system. In collision the bunch length cannot be increased beyond about  $\sigma_L \approx \beta^*$  without the loss of luminosity to the “hourglass” effect.

### 4 ELECTRON STORAGE RING ISSUES

**Synchrotron radiation.** The synchrotron radiation energy loss per electron per turn of a storage ring with dipoles of bending radius  $\rho$  is

$$U_0 [\text{MeV}] = 0.0885 \frac{E^4 [\text{GeV}^4]}{\rho [\text{m}]} \quad (12)$$

and the total power radiated is

$$P [\text{MW}] = U_0 [\text{MeV}] I [\text{A}] \quad (13)$$

One constraint on the maximum beam current in the SLAC B-Factor High Energy Ring (HER) is the need to keep the linear heat load per meter of dipole, given by

$$P_{lin} = \frac{P}{2\pi\rho} \quad (14)$$

to less than about 15 kW/m [9, 16]. The HER serves as a natural “ruler” against which to compare prospective electron ring parameters. For example, Table 1 shows that, with 360 bunches, the eRHIC bunch spacing of 35.5 ns is modest by comparison with the HER, which has as many as 1658 bunches, with a bunch spacing as small as 4.2 ns. Thus, the synchrotron power and linear power in the arcs are much less in the eRHIC ring than in the HER.

**Polarization.** The natural Sokolov-Ternov polarization time for electrons stored in a ring is

$$T_{pol} [\text{s}] = 15.8 \frac{C \rho^2 [\text{m}^3]}{E_e^5 [\text{GeV}^5]} \quad (15)$$

This can be very long – for example, 9.9 hours in a full circumference eRHIC electron ring! Further, it is not possible to accelerate (or decelerate) electrons through intrinsic spin resonances, which are located at energies given by

$$E_{\text{resonance}} = J 0.441 \text{ [GeV]} \quad (16)$$

where  $J$  is an integer. In this case full energy electrons must be injected pre-polarized. It is natural to consider using permanent magnet technology for some or most of the ring lattice magnets in such a fixed energy ring. One way to inject full energy pre-polarized electrons is to use a full energy linac equipped with a polarized source. Another is to use a conventional booster ring. Equation 15 shows that an eRHIC booster with 1 T dipoles ( $\rho = 33.4$  m) and a packing fraction of 0.5 ( $C = 420$  m) has a polarization time of only  $T_{\text{pol}} = 74$  s. Such a booster would accelerate electron bunches from (say) a 1 GeV injection energy to a 10 GeV flat-top, and then hold them there for a couple of minutes, before injection into the electron storage ring.

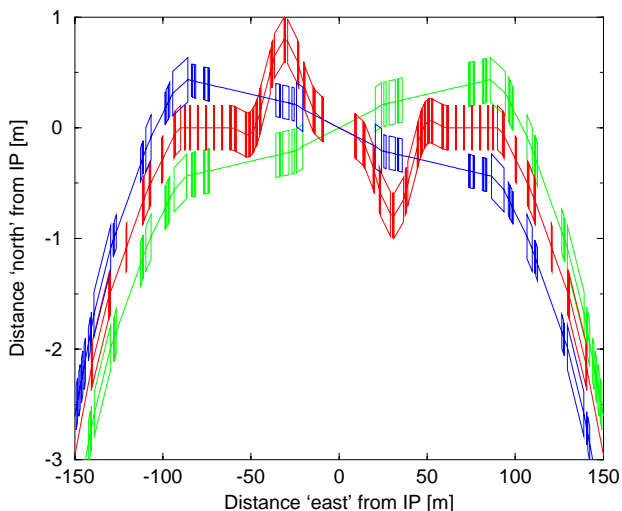


Figure 2: Plan view of an eRHIC IR with spin rotators.

**Interaction Region optics – spin rotators.** In some cases it may not be necessary to provide longitudinally polarized electrons at the IP. In this case the interaction region optics are relatively attractive, because weaker dipole fields are permitted, with lower synchrotron radiation linear power loads. Polarized electron experiments require the spin vector to be longitudinal at the IP, while the spin vector is naturally vertical in the arc of a ring. The transformation from vertical to longitudinal polarization (and back again) is achieved by including spin rotators in the interaction region optics. Figure 2 shows a straw man eRHIC interaction region layout, including spin rotators [5]. Not shown in the plan view is a vertical drop of almost 1 m, which puts the electron ring near the floor of the tunnel in the arcs. The spin rotator dipoles may have much higher fields than in the arcs – as high as  $B = 0.43$

T in the straw-man eRHIC optics. These few dipoles have much higher linear heat loads than the common arc dipoles.

## 5 ENERGY RECOVERY LINAC ISSUES

The natural potential advantages of a linac-ring collider stem from the single pass nature of the beam. Not only do the electrons collide with the ion beam with the initial properties of the linac (rather than the equilibrium values of a ring), but it is also possible to exceed the multi-turn dynamical limits of a ring. The linac generates a low emittance beam with a low energy spread, leading to a small collision point beam size with a relatively large beta function that simplifies the interaction point optics. The beam is naturally round, as is the ion beam. If collisions are required at only one IP, then there is no need for a spin rotator in the IR optics, since the electron beam polarization vector can be prepared with the correct orientation close to the source of the linac. A single pass collider can provide a polarized electron beam energies over a relatively broad range, while a storage ring must avoid spin resonances. It should be possible to alternate the sign of the polarization in a linac rapidly, at will. Linac-ring collisions increase the maximum permissible value of  $\xi_e$ , the electron beam-beam parameter – the electron beam can be “destroyed” by beam-beam forces, and still have its energy recuperated. Equation 4 shows that this allows the number of ions per bunch  $N_i$  and  $\beta_e^*$  to be increased, and permits smaller emittance ion beams, attained for example through the use of electron cooling.

**Energy recuperation.** With typical average electron beam powers of order 1 GW, the recovery efficiency of an ERL must be very high in order to avoid excessive power budgets. This requires the use of a superconducting linac. Energy recovery has already been successfully demonstrated at the Jefferson National Accelerator Facility IR-FEL facility, albeit with low power, current, and energy (250 kW, 5 mA, and 50 MeV) [17, 18]. Several indicators at the JLab IR-FEL place an upper limit on the beam loss at  $2\mu\text{A}$ , or  $\sim 4 \times 10^{-4}$ , an extremely small value [19]. In a high power electron-ion collider ERL, fractional beam losses at this upper limit could be unacceptable, since they potentially give rise to hundreds of kW of uncontrolled beam power losses. Very little power can be lost at cryogenic temperatures. More work is required to understand both the origin of ERL beam losses, and their possible cures.

In order to avoid beam-beam collisions of the accelerated and decelerated beam, the two beams must propagate in the same direction of the linac [20]. Thus the transverse optics at each end of the linac must deal with beams of very different energies. The energy difference should be no more than about a factor of 10 – or perhaps much more [21]. Since the energy recuperation must go down to a low energy, multiple stages may be required. A straw man four stage scheme is shown conceptually in Figures 3.

A 10 GeV ERL would be about 500 meters long, using TESLA cavities at an average gradient of 20 MV/m. The first acceleration section invests 1.35 MW (at 0.135 A) in the 10 MeV beam, with no recuperation. The returning 10 MeV beam is sent to a beam dump. Next is a low gradient 90 MeV (energy gain) section, where energy recuperation is performed in a separate dedicated RF structure. The recovered energy is fed through waveguides to the accelerating section. Third, the 100 MeV beam acquires 0.9 GeV from an intermediate linac also performing energy recovery. Last is the main linac, with an energy gain of 9 GeV. The 10 GeV beam is taken to the collision point.

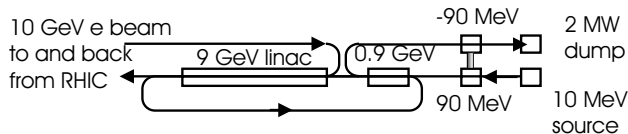


Figure 3: Concept of a four stage Energy Recovery Linac, in the linac-ring collision scenario.

**Beam transport.** Figure 1 (BOTTOM) sketches the layout of a four stage ERL with a “full radius” recirculator, in which the returning 10 GeV beam bends through dipoles with the same radius as the ion ring dipoles (or electron storage ring dipoles). The total and linear synchrotron power loads are somewhat lower than they would be in an electron storage ring, by the ratio of the beam currents – as much as a factor of 3 for eRHIC, according to Table 1. However, Equations 12 to 14 show that this significant advantage is eroded if the bending radius of curvature is much reduced. The minimization of undesirable synchrotron radiation is a distinct advantage of a “full radius” recirculator, even if collisions are only required at a single IP.

**Higher Order Mode power dissipation.** Next to beam loss, the most serious issue is that of collective beam instabilities driven by Higher Order Modes (HOMs) of the Superconducting RF (SRF) cavities. The HOM power depends on the product of the bunch charge and the average current. In the EPIC case (with an average current of 0.264 A) approximately 8 kW of HOM power is dissipated per cavity, primarily in longitudinal modes. Fortunately, an analytical model [22] predicts that only a few Watts of this power is deposited on the cavity walls, at cryogenic temperatures. Engineering studies on cooled HOM absorbers placed between cavities or cryomodules are called for [19].

**Beam Break Up.** Collective Beam Break Up (BBU) phenomena can limit the linac performance both longitudinally and transversely, single and multi-bunch, and single pass and multiple pass. Single bunch effects include energy spread induced by longitudinal wakefields, and emittance growth driven by transverse wakefields. Multi-bunch, multi-pass BBU occurs when recirculating a beam through a (high  $Q$  superconducting) cavity leads to a transverse in-

stability. The recirculated beam and a transverse deflecting HOM form a “feedback” loop which goes unstable, beyond a threshold current that depends on various cavity and lattice parameters. The two dimensional code TDBBU [8, 23] has been used to calculate the threshold current in EPIC and eRHIC machine configurations, using published TESLA HOM data [24]. In both cases the predicted thresholds, while impressively high (205 mA and 100 mA), are somewhat below the average currents shown in Table 1. In the eRHIC case the 100 MeV to 1 GeV linac section was the most vulnerable. These threshold currents apply in the absence of feedback. Typical instability growth times, just above threshold, are in the millisecond range. Hence, with feed back, it should be possible to go to even higher average currents.

## 6 ACKNOWLEDGEMENTS

Sincere thanks go to L.Merminga, for her support.

## 7 REFERENCES

- [1] A.De Roeck, D.Barber, G.Rädel, eds., DESY-PROC-1999-03.
- [2] The first eRHIC workshop, <http://www.star.bnl.gov/afs/rhic/star/doc/www/collab/erhic/erhic.html> BNL, 1999.
- [3] The second eRHIC workshop, [http://quark.phy.bnl.gov/~raju/yale\\_eRHIC.html](http://quark.phy.bnl.gov/~raju/yale_eRHIC.html) Yale, 2000.
- [4] Part VI, TESLA Technical Design Report, 2001.
- [5] I.Ben-Zvi et al, accepted for NIM A, 2001.
- [6] The second EPIC workshop, MIT, 2000.
- [7] C.Sinclair, p. 65, PAC 1999.
- [8] D.Engwall et al, p. 2693, PAC 1997.
- [9] J.Seeman, p.1, PAC 1999.
- [10] P.Cameron, M.Morvillo, RHIC/AP/68, BNL, 1996.
- [11] F.Zimmerman, LHC Project Report 95, 1997.
- [12] O.Gröbner, PAC 1997.
- [13] O.Brüning, LHC Project Report 102, 1997.
- [14] W.MacKay et al, these proceedings.
- [15] I.Ben-Zvi et al, these proceedings.
- [16] “Asymmetric B Factory Design Report”, SLAC 372, 1991.
- [17] P.Grosse-Wiesmann, SLAC-PUB-4545, 1988.
- [18] J.Bisognano et al, p. 586, LINAC 1988.
- [19] L.Merminga et al, HEACC 2001.
- [20] D.Douglas, JLAB-TN-98-040, 1998.
- [21] I.Bazarov, these proceedings.
- [22] L.Merminga et al, LINAC 2000.
- [23] G.Krafft, J.Bisognano, p. 1356, Proc. PAC 1987.
- [24] J.Sekutowicz, TESLA 94-07, 1994.